

Manuscript Details

Manuscript number	JCOMB_2018_1506
Title	A NEW STRENGTHENING TECHNIQUE FOR INCREASING THE LOAD CARRYING CAPACITY OF RECTANGULAR REINFORCED CONCRETE COLUMNS SUBJECTED TO AXIAL COMPRESSIVE LOADING
Article type	Full Length Article

Abstract

In this work, a new technique for the efficient confinement of reinforced concrete (RC) columns of rectangular cross-section is described and its effectiveness is assessed experimentally. This technique is based on the concept of applying strips of carbon fiber reinforced polymer (CFRP) wet layup sheets with a certain prestress level using a mechanical device. The influence of the cross-section aspect ratio of columns on the axial stress-strain response, strain field in the CFRP and strength increase provided by the different adopted strengthening configurations was investigated. All specimens had a height of 1100 mm, and three cross-sections were considered: 120 mm×120 mm, 240 mm×120 mm and 480 mm×120 mm, representing cross-section aspect ratios (large/small edge) equal to 1, 2 and 4, respectively. Four types of columns were tested: conventional RC columns (reference columns), fully-wrapped columns, partially-wrapped columns, and columns strengthened according to the new technique. All columns were subjected to axial compression loading until failure. The experimental results show that the cross-section aspect ratio has a significant effect on the confinement effectiveness that CFRP strengthened systems can provide to RC columns of rectangular cross-section. The maximum axial strength and axial strain at the peak load of all columns significantly decrease when the cross-section aspect ratio increases. Based on the obtained experimental results, it is shown that the proposed technique is more efficient in terms of increasing the load carrying capacity of rectangular RC columns than CFRP-based conventional strengthening techniques.

Keywords	Confinement, RC columns of rectangular cross-section, CFRP, Prestress application, Axial compressive loading tests, Analytical model
Manuscript region of origin	Europe
Corresponding Author	Worajak Janwaen
Corresponding Author's Institution	University of Minho
Order of Authors	Worajak Janwaen, Joaquim Barros, Inês Costa
Suggested reviewers	Nicola Nistico, Omar Chaallal, Theodoros Rousakis

Submission Files Included in this PDF

File Name [File Type]

CoverLetter_CompositesPartB.docx [Cover Letter]

Highlights_CompositesPartB.docx [Highlights]

JanwaenEtAl_Text.docx [Manuscript File]

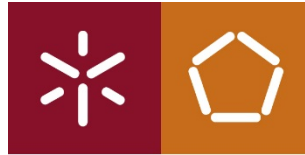
JanwaenEtAl_Figures.docx [Figure]

JanwaenEtAl_Tables.docx [Table]

To view all the submission files, including those not included in the PDF, click on the manuscript title on your EVISE Homepage, then click 'Download zip file'.

Research Data Related to this Submission

There are no linked research data sets for this submission. The following reason is given:
Data will be made available on request



Universidade do Minho
Escola de Engenharia

To the Editor of the Composites Part B:
Engineering Journal

May 18, 2018

Dear Editor,

I am submitting an original research article entitled “A NEW STRENGTHENING TECHNIQUE FOR INCREASING THE LOAD CARRYING CAPACITY OF RECTANGULAR REINFORCED CONCRETE COLUMNS SUBJECTED TO AXIAL COMPRESSIVE LOADING” for consideration of publication in the Composites Part B: Engineering Journal.

This manuscript describes the development of a new innovative technique based on the concept of applying strips of carbon fiber reinforced polymer (CFRP) wet layup sheets with a certain prestress level using a mechanical device for increasing the load carrying capacity of rectangular reinforced concrete (RC) columns. In this scientific subject, the experimental tests are performed and compared with the conventional strengthening techniques (full and partial confinement techniques). The applicability of the ACI, *fib* Bulletin 14 and CNR-DT 200 guidelines is also assessed for the prediction of the compressive strength of columns confined with FRP systems. It is concluded that the new technique is more efficient in terms of increasing the load carrying capacity of rectangular RC columns than CFRP-based conventional strengthening techniques. Finally, the design guidelines are adapted for estimating the compressive strength of rectangular cross section RC columns strengthened according to the new technique, and good predictive performance was obtained.

This manuscript describes the Authors’ original work. It has not been published elsewhere and is not under consideration by another journal. The authors approved the manuscript and agree with this submission. No conflict of interest to declare.

Thank you very much for your consideration of this manuscript.

Yours Sincerely,

Worajak JANWAEN

Worajak Janwaen
(Corresponding Author)

PhD Candidate, ISISE, Department of Civil Engineering, University of Minho
Campus de Azurém, 4800-058, Guimarães, Portugal

Email: tontrakarn.w@gmail.com

Highlights

- A new technique (SC) for the confinement of RC columns of rectangular cross-section is proposed
- The efficiency of the SC technique was experimentally compared with FRP-based existing ones
- The proposed SC technique was more efficient than the fully- and partially-wrapped techniques
- Guidelines were adapted for predicting the strength of RC columns confined with the SC technique
- Good predictive performance was obtained for the proposed design guideline

1 **A NEW STRENGTHENING TECHNIQUE FOR INCREASING THE LOAD CARRYING**
2 **CAPACITY OF RECTANGULAR REINFORCED CONCRETE COLUMNS SUBJECTED**
3 **TO AXIAL COMPRESSIVE LOADING**

4
5 Worajak Janwaen^a, Joaquim A. Barros^b and Inês G. Costa^c

6
7 ^aPhD Candidate, ISISE, Department of Civil Engineering, University of Minho, Azurém 4800-058
8 Guimarães, Portugal, tontrakarn.w@gmail.com (corresponding author)

9 ^bFull Prof., ISISE, Department of Civil Engineering, University of Minho, Azurém 4800-058
10 Guimarães, Portugal, barros@civil.uminho.pt

11 ^cPhD Civil Eng., CiviTest, Parque Industrial de Jesufrei, Rua da Indústria, n.º144, 4770-160 Vila
12 Nova de Famalicão, Portugal, inescosta@civitest.com

13
14
15 **Abstract**

16 In this work, a new technique for the efficient confinement of reinforced concrete (RC) columns of
17 rectangular cross-section is described and its effectiveness is assessed experimentally. This technique
18 is based on the concept of applying strips of carbon fiber reinforced polymer (CFRP) wet layup sheets
19 with a certain prestress level using a mechanical device. The influence of the cross-section aspect
20 ratio of columns on the axial stress-strain response, strain field in the CFRP and strength increase
21 provided by the different adopted strengthening configurations was investigated. All specimens had a
22 height of 1100 mm, and three cross-sections were considered: 120×120 mm², 240×120 mm² and
23 480×120 mm², representing cross-section aspect ratios (large/small edge) equal to 1, 2 and 4,
24 respectively. Four types of columns were tested: conventional RC columns (reference columns), fully-
25 wrapped columns, partially-wrapped columns, and columns strengthened according to the new
26 technique. All columns were subjected to axial compression loading until failure. The experimental
27 results show that the cross-section aspect ratio has a significant effect on the confinement
28 effectiveness that CFRP strengthened systems can provide to RC columns of rectangular cross-
29 section. The maximum axial strength and axial strain at the peak load of all columns significantly
30 decrease when the cross-section aspect ratio increases. Based on the obtained experimental results, it
31 is shown that the proposed technique is more efficient in terms of increasing the load carrying
32 capacity of rectangular RC columns than CFRP-based conventional strengthening techniques.

33
34 **Keywords:** Confinement, RC columns of rectangular cross-section, CFRP, Prestress application,
35 Axial compressive loading tests, Analytical model

36
37
38
39
40
41
42
43
44
45
46
47
48
49
50
51
52
53
54
55
56
57
58
59
60
61
62
63
64
65
66
67
68
69
70
71
72

1. INTRODUCTION

In recent years, Fiber Reinforced Polymer (FRP) composites have been extensively used for the strengthening and rehabilitation of existing reinforced concrete (RC) structures. There are several reasons for using FRP composites, such as high stiffness, lightweight, non-corrosiveness in harsh environments, and the ease of application [1]. Externally bonded FRP composite jacketing is one of the most common applications of FRP composites for the strengthening of RC columns as it can provide significant confinement to the concrete, mainly in columns of circular cross-section. This technique allows the increase of axial load and deformation capacity, as well as its energy absorption performance [2].

From previous studies, it can be clearly noted that the confinement effectiveness depends on the lateral confining pressure applied to the concrete core. The confinement of FRP-strengthened columns with circular section is more efficient than in columns with non-circular section due to the uniform confining pressure assured by the former type of cross-section [3-8]. However, most of the existing structural columns have a rectangular cross-sectional configuration. Relatively less experimental data exists on RC columns of rectangular cross-section confined with FRP systems, and, hence, the availability of reliable models for the prediction of their response is limited [6, 9-10]. Mirmiran *et al.* [3] studied the confinement of concrete columns of circular and square cross-sections with FRP jackets and found that its effectiveness depends on several parameters such as concrete strength, type of fibers and resins, fiber volume and fiber orientation in the jacket, jacket thickness, shape of cross-section (circular versus square), slenderness ratio of the column (i.e. length-to-diameter/edge ratio) and the interface bond between the core and the jacket. Other research works also found that the corner radius of FRP-confined prismatic concrete columns is an important parameter that influences the confinement effectiveness of FRP strengthening systems [3, 11-15]. This issue is attributed to the stress concentration occurring in the corner zones, which promotes premature tensile rupture of the strengthening systems, particularly if the corner radius is less than a critical value [3, 11-15]. Moreover, the size and aspect ratio of the cross-section (largest edge to smallest edge ratio) can also compromise the effective confinement provided by FRP systems. When this aspect ratio increases, the confinement effectiveness of the columns significantly decreases [16-17]. To improve the efficiency of FRP confined columns, the use of hybrid strengthening techniques has been previously explored. Hadi *et al.* [18] used a technique that converts a square column to a circular section by bonding pieces of segmental circular concrete covers, called the Circularization technique, providing a significant increase of the confinement effectiveness of the column. However, the geometry of these columns can be significantly altered, the intervention can be quite time consuming, and the confinement effectiveness is susceptible to the creep of the segmental circular concrete covers. Rousakis and Tourtouras [19] proposed a strengthening technique for RC columns of square cross-section by using special mechanical devices combined with highly deformable polypropylene fiber ropes, PPFR. The

73 results revealed that the stress-strain relationship of the strengthened columns was highly improved by
74 the proposed technique, having the strengthened RC columns exhibited higher load carrying capacity
75 when compared to columns with conventional wrapping techniques. Nevertheless, the technique
76 requires a high content of wrapping material to ensure proper strengthening conditions for applying
77 the prestress to the PFR system.

78 In the present work, a new strengthening technique is proposed for increasing the axial load carrying
79 capacity and deformation performance of RC columns of rectangular cross-section. This strategy,
80 herein denominated by strip constriction (SC) technique, is based on the concept of applying strips of
81 carbon fiber reinforced polymer (CFRP) wet layup sheets with a certain prestress level by means of a
82 mechanical device. The influence of cross-sectional aspect ratio of columns on the confinement
83 behavior was investigated. The performance of the SC technique is compared to the one provided by
84 conventional strengthening techniques based on the full or partial confinement of the columns with
85 CFRP wet layup sheets. In the following sections, the experimental program is detailed, and the
86 relevant results are presented and discussed.

87 The applicability of ACI [1], *fib* Bulletin 14 [21] and CNR-DT 200 [22] guidelines for the prediction
88 of the compressive strength of columns confined with FRP systems is assessed. Finally, these
89 guidelines are improved in order to be capable of predicting with acceptable accuracy the load
90 carrying capacity of RC columns confined with the new proposed technique.

91

92 **2. EXPERIMENTAL PROGRAM**

93 **2.1 Column prototypes**

94 The experimental program includes a total of 11 prototypes of column to investigate the compressive
95 behavior of rectangular RC columns externally confined by CFRP wet layup sheets (Fig. 1). All
96 specimens have 1100 mm in height, and all strengthened columns have a corner radius of 25 mm to
97 minimize premature failure occurrence in the CFRP due to high tensile stress developments in these
98 zones. Different types of CFRP strengthening techniques and arrangements, and different aspect ratio
99 for the cross-section of the columns, were considered for investigating their influence on the
100 strengthening performance. Four types of RC columns were executed: (1) Without any type of
101 strengthening intervention, considered the reference columns (REF); (2) Fully-wrapped columns
102 (FW); (3) Partially-wrapped columns (PW); (4) Columns strengthened according to the new technique
103 (SC). The cross-sections of the columns investigated in this experimental program were 120×120
104 mm², 240×120 mm² and 480×120 mm², representing a cross-section aspect ratio (larger/smaller edge,
105 $\lambda=h/b$) of, respectively, 1, 2 and 4. All strengthened columns were confined using three layers of
106 CFRP sheet. To prevent failure due to stress concentration in the extremities of the columns in contact
107 with the test equipment, two additional strips of 90 mm width were applied in the zones, resulting in
108 five layers of CFRP sheet.

109 The strengthening according to the new technique (SC) was performed using a mechanical device
110 detailed in Figs. 1-2. The mechanical device consists of two parts: two D-shaft round (D-shaped) steel
111 bars (with a diameter of 50 mm) with one hole to insert a threaded rod; and a threaded rod with
112 washer and nut. The D-shaped devices are later fastened against the CFRP strips using a washer and
113 nut on the opposite extremity, transmitting the intended prestress level to the CFRP strips, which
114 introduces an initial confinement stress field in the RC column.

115 The columns are labeled as " $\lambda X-Y$ ", where λ represents the cross-section aspect ratio (h/b) and
116 therefore X can assume the values of 1, 2 and 4; Y is replaced by REF, FW, PW, SC for representing
117 the reference column, the column fully wrapped, the column partially wrapped and the column
118 strengthened according to the strip constriction technique. For example, $\lambda 2-FW$ is the column with a
119 cross-section aspect ratio of 2, and fully wrapped.

120

121 **2.2 Material properties**

122 **2.2.1 Concrete**

123 Local Portland cement, river sand, and coarse aggregate of 12 mm maximum size were used for
124 producing the concrete of the columns. The average compressive strength of 4 cylindrical concrete
125 specimens of 150 mm diameter at 28 days was 21 MPa (with COV of 2.8%), obtained by performing
126 compression tests according to the BS EN 12390-3:2009 recommendations [20].

127

128 **2.2.2 Reinforcement**

129 For the reinforcement of the columns, ribbed bars of 6 mm diameter were used as steel hoops, and
130 10 mm diameter as longitudinal bars. The nominal yield stress of the reinforcement was
131 approximately 550 and 450 MPa for the ribbed bars of 6 and 10 mm, respectively.

132

133 **2.2.3 CFRP sheets**

134 A high tensile strength carbon fiber fabric, S&P C-sheet 240 was used for wrapping the columns.
135 Two-component S&P epoxy resin 55 was used to impregnate the CFRP sheets. The details of CFRP
136 material properties from the technical data sheet are shown in Table 1.

137

138 **2.3 Preparation of column prototypes**

139 **2.3.1 CFRP Wrapping**

140 For wrapping the columns, the procedure recommended by ACI 440.2R-08 [1] was followed. The
141 corners of the cross-section were grinded up to the desired radius of 25 mm, and the concrete surface
142 to be in contact with the CFRP was lightly sanded to smoothen the surface. Water was used to remove
143 all dust and dirt from the surface, and the columns were then left to dry. When necessary, voids on the
144 surface of columns were filled using cement paste. A two-component epoxy resin was used to bond

145 the CFRP sheets to the surface of the columns. The relevant properties of epoxy resin are also
146 indicated in Table 2. Before placing the CFRP sheets, a thin layer of resin was applied on the surface
147 of the columns. The first layer of CFRP sheet was then placed on the surface of the columns. A plastic
148 roller was used to remove the excess resin and any air voids between the CFRP layer being applied
149 and the substrate. For wrapping subsequent layers, the epoxy resin was applied again on the outer
150 surface of the previous layer, and the next layer of CFRP sheet was placed. On each CFRP layer, an
151 overlap of 50 mm was ensured. The CFRP wrapping system was arranged in order to become
152 symmetric in parallel to the longer edge of the cross-section. After placing the last layer of CFRP, a
153 final coat of epoxy resin was applied, and the plastic roller was used once again in an attempt of
154 removing air voids. Finally, the wrapped columns were left to dry in laboratory environment for
155 approximately one week before testing.

156

157 ***2.3.2 The proposed strip constriction (SC) technique***

158 Before applying the CFRP strips, a transparent plastic-film was applied on the concrete column to
159 reduce the friction between the concrete surface and the CFRP strips. The CFRP strips were then
160 bonded by ensuring an overlapping length of approximately 50 mm at one of the shorter sides of the
161 column's cross-section, and left to dry for approximately one week. In order to transfer the intended
162 prestress to the CFRP strips (approximately 20% of the ultimate strain of the CFRP sheet), the
163 previously presented mechanical system was used. To install the device, firstly, the threaded rod was
164 inserted through a hole previously drilled on the column. Then, the D-shaped steel bars were installed
165 on both sides of the column. Finally, a nut was gradually screwed with a dynamometric wrench. In
166 each turn, the D-shaped steel bars push the CFRP strips into the grooved section, inducing the
167 intended prestress in the CFRP strips. The torque from the wrench and the strain of the CFRP strips
168 were monitored up to the attainment of the target strain in the CFRP strips (0.33%). The above
169 indicated plastic-film applied in the contact zones between CFRP strips and concrete substrate has the
170 purpose of promoting as much as possible a uniform prestress distribution on the column perimeter.
171 The prestress application on the CFRP strips is illustrated in Fig. 3.

172

173 **2.4 Testing instrumentation**

174 All columns were capped with polyester paste on the bottom and top surface of the columns for
175 promoting uniform axial load transference. Additionally, a plastic film with oil was applied at both
176 ends of the columns, between the surface of the concrete and the testing frame to further reduce the
177 surface friction. Strain gauges (SG) were installed in the strengthened columns, at mid-height, to
178 monitor the strain evolution in different positions. One strain gauge was installed at the center of the
179 shorter edge, while other(s) was(ere) placed along the longer side of the column's cross-section
180 according to the schematic representation in Fig. 4.

181 Linear voltage displacement transducers (LVDTs) were also installed to record the axial deformation
 182 of the columns. Three different distances along the column height were monitored to evaluate the
 183 overall behavior of the columns. The selected distances between the lower and upper fixing points
 184 were 1060 mm, 600 mm and 200 mm (Fig. 4). The columns were subjected to direct axial
 185 compression by means of a closed loop servo-controlled actuator equipped with a load cell of
 186 2000 kN capacity. By reading the LVDTs located symmetrically on the outer sides of the columns, it
 187 was verified that an almost pure axial load was assured up to 20% of peak load in the pre-peak stage.
 188 Above the deformation corresponding to this load level, parasitic bending moments are introduced
 189 due to the non-uniform damage occurring in the cross-section, fundamentally caused by the non-
 190 homogeneous material nature of concrete. A representation of the instrumentation of the column
 191 prototypes is shown in Fig. 4.

192

193 3. EXPERIMENTAL RESULTS AND DISCUSSION

194 3.1 Overall behavior

195 The summary results obtained from the experimental tests are presented in Table 3. In this table, A_{eff}
 196 is the effective column's cross-section (after the treatment for the strengthening process); P_{max} is the
 197 maximum load supported by the column; σ_{cc} is the axial stress at P_{max} ($\sigma_{cc} = P_{max} / A_{eff}$); ε_{cc} is the
 198 axial strain (measuring stroke of 1060 mm) at P_{max} ; $\varepsilon_{f_{max}}$ is the maximum strain in the CFRP
 199 recorded up to the end of the tests; $\Delta F_{max} = 100 \times (P_{max}^{Str} - P_{max}^{Ref}) / P_{max}^{Ref}$ represents the increase of load
 200 carrying capacity provided by the strengthening technique, where P_{max}^{Str} and P_{max}^{Ref} are the maximum
 201 load of the strengthened and its corresponding reference column; $\overline{\Delta \varepsilon_{cc}} = 100 \times (\varepsilon_{cc}^{Str} - \varepsilon_{cc}^{Ref}) / \varepsilon_{cc}^{Ref}$ is
 202 the increase of axial strain at P_{max} , where ε_{cc}^{Str} and ε_{cc}^{Ref} are the axial strain of the strengthened
 203 column and its corresponding reference column at P_{max} ; and $\Delta F_{max} / A_{CFRP}$ is the increase of load
 204 carrying capacity per quantity of CFRP strengthening material, where A_{CFRP} is the total area of CFRP
 205 sheet applied in a strengthened column. It can be seen that the columns strengthened with
 206 conventional CFRP techniques (fully and partially wrapped), apart the case of $\lambda 1$ -FW, have provided
 207 a modest increase in terms of strength gain (ΔF_{max}). However, the columns strengthened according to
 208 the strip constriction (SC) technique showed a higher strength gain, and the confinement effectiveness
 209 seems to increase with the column's cross-section aspect ratio (λ). In fact, while the SC technique
 210 provided an increase of ΔF_{max} from 25% to 32% with the increase of the cross-section aspect ratio
 211 from 2 to 4, the fully and partially wrapped techniques provided a decrease from 23% to 7% and from
 212 13% to 10%, respectively.

213

214 **3.2 Failure modes**

215 The failure mechanisms of the columns were monitored throughout the experimental tests. It was
216 found that the variation of the cross-section aspect ratios showed no significant effect on the typical
217 failure modes of the columns. The failures of the columns consisted of one or both of the two
218 following types: (1) crushing-splitting of concrete; and (2) rupture of CFRP layers. In the reference
219 columns ($\lambda 1$ -REF, $\lambda 2$ -REF and $\lambda 4$ -REF), failure almost coincided with the attainment of the
220 column's maximum load capacity. The failure occurred suddenly accompanied by an explosive
221 spalling of concrete, followed by the buckling of longitudinal reinforcing bars. The failure regions
222 were very close to the extremities of the columns due to the high stress concentration in these regions.
223 Therefore, despite the one extra steel hoop (at 25 mm from the regular one) applied in these regions in
224 all the tested columns (Fig. 1), it was not possible to avoid this type of failure in the REF columns. In
225 Figs. 5a, 6a and 7a, it can also be noted that the failure took place between the steel hoops. The
226 detachment of the concrete cover has favored the occurrence of buckling of the longitudinal
227 reinforcing bars leading to the collapse of the columns. It can also be mentioned that bar buckling
228 mostly occurred along the shorter side of the column section. Nevertheless, the bar buckling of $\lambda 4$ -
229 REF could be observed in both shorter and longer sides of the column (Fig. 7a).

230 Regarding the fully-wrapped columns ($\lambda 1$ -FW, $\lambda 2$ -FW and $\lambda 4$ -FW), all columns failed by CFRP
231 rupture as illustrated in Figs. 5b, 6b and 7b. This failure also occurred suddenly, accompanied by an
232 explosive sound at the moment of the CFRP rupture. The rupture of the CFRP layers occurred near
233 the directly loaded zone (upper extremity) of the columns $\lambda 2$ -FW and $\lambda 4$ -FW, while in the $\lambda 1$ -FW
234 column it has occurred at mid-height. Regarding the $\lambda 4$ -FW column, the observed abrupt load decay
235 just after the peak load was caused by the concrete core crushing. The concrete expansibility caused
236 by this crushing process has significantly mobilized the CFRP wrapping mechanism, which was
237 capable of maintaining the load carrying capacity almost constant up to an axial strain of 3%, when
238 the CFRP failed in tension. When the confinement effectiveness of the fully-wrapped columns was no
239 longer provided by CFRP sheets, the concrete started spalling, followed by the buckling of
240 longitudinal reinforcing bars between the steel hoops. The CFRP tensile rupture was followed by the
241 detachment of the CFRP from the surface of the columns.

242 The partially-wrapped columns ($\lambda 1$ -PW, $\lambda 2$ -PW and $\lambda 4$ -PW) gradually lost their load carrying
243 capacity with the increase of the axial deformation above the strain at peak load, which was caused by
244 the progressive concrete crushing and buckling of the longitudinal bars at the unwrapped zones. This
245 progressive damage process has ended with the CFRP tensile rupture of the top group of strips in the
246 $\lambda 2$ -PW and $\lambda 4$ -PW columns, followed by the spalling of concrete in the wrapped zones where this
247 failure has occurred (Figs. 6c and 7c). In the $\lambda 1$ -PW column, an intense curvature has occurred in the

248 first unwrapped zone from the top surface of this column, without any occurrence of CFRP tensile
249 rupture (Fig. 5c).

250 In the columns strengthened according to the new technique (λ 2-SC and λ 4-SC), failure took place
251 noisily due to the rupture of CFRP strips in the zones contacting the mechanical device (Figs. 6d and
252 7d). After the CFRP rupture, the load carrying capacity of λ 2-SC has gradually decreased by concrete
253 crushing up to the end of the test (Fig. 6d). The λ 4-SC column suddenly failed by an explosive
254 crushing of concrete, and the test was stopped by the loading machine control software. It was
255 verified that the concrete core of this column was completely damaged due to the explosive nature of
256 the failure (Fig. 7d). The failure region was localized at the top extremity of the column (the one in
257 direct contact with the hydraulic jack). Moreover, the longitudinal bars have buckled in this localized
258 damage zone.

259

260 **3.3 Stress-strain response**

261 The stress-strain relationship of the RC tested columns is shown in Figs. 8-9. The axial stress was
262 calculated as the ratio between the applied force and the effective cross-sectional area of the column (
263 $\sigma_c = P/A_{eff}$). The axial strain was determined by dividing the average displacement readings of the
264 LVDTs by the corresponding measuring stroke, having been adopted three values for the measuring
265 stroke (200, 600 and 1060 mm, Fig. 4) for assessing its influence on the column's axial strain. The
266 results presented in Fig.8, corresponding to the λ 1-REF column, can be considered representative of
267 the columns of the experimental program. This stress-strain graph demonstrates that, up to peak load,
268 the column's axial strain is almost the same regardless of the measuring stroke considered to convert
269 the displacements recorded in the LVDTs in strains. The strains only become dependent of the
270 measuring stroke when a localized failure starts.

271 Fig. 9 shows the relationship in terms of axial stress versus axial strain (adopting the measuring stroke
272 of 1060 mm for the determination of the strain values) for all the tested columns.

273 All reference columns (λ 1/2/4-REF) showed a very brittle behavior, as is shown from their
274 stress-strain relationship, since failure was caused by concrete spalling. Regarding the strengthened
275 columns, all of them presented an increase in terms of load carrying capacity and axial deformability,
276 due to the confinement effectiveness provided by the CFRP systems. In the fully-wrapped columns,
277 the one with a cross-section aspect ratio of 1 (λ 1-FW) developed a pronounced hardening stage up to
278 the CFRP tensile failure; the column of λ =2 (λ 2-FW) presented an almost "pseudo-rigid-plastic
279 behavior", and the column of λ =4 (λ 4-FW) experienced a significant drop of load carrying capacity
280 just after the peak load. Therefore, by increasing λ , the confinement performance of the FW group of
281 columns has decreased in terms of compressive strength and deformation capability. The hardening
282 and almost "pseudo-rigid-plastic" stages verified in λ 1-FW and λ 2-FW, accompanied by a relatively
283 large axial deformability, is a consequence of the effective activation of the confinement pressure

284 provided by the CFRP systems. The level of confinement effectiveness was much lower in the $\lambda 4$ -FW
285 column, as consequence of the smaller stiffness of this CFRP arrangement, allowing a higher concrete
286 expansibility during concrete core crushing, which led to the tensile rupture of the CFRP.

287 Regarding the partially-wrapped columns ($\lambda 1$ -PW, $\lambda 2$ -PW and $\lambda 4$ -PW), a softening branch was
288 clearly visible on the stress-strain curves after the maximum load had been attained. However, due to
289 the confinement provided by the CFRP strips, the post-peak load carrying capacity of these columns
290 did not suddenly drop. The gradual stress decay in these columns was mainly caused by the damage
291 evolution occurred in the concrete volume in-between the first two sets of CFRP strips from the
292 loading extremity of these columns.

293 For the columns strengthened according to the proposed technique, $\lambda 2$ -SC developed the highest first
294 peak load. However, due to the pronounced damage evolution of the concrete volume in-between the
295 first two sets of CFRP strips from column's loading extremity (Fig. 6d), its loading carrying capacity
296 has gradually decreased. At about 4.5% of axial deformation, the post-peak compressive stress is the
297 same as in the fully wrapped column ($\lambda 2$ -FW). Regarding the series of columns with the highest
298 cross-section aspect ratio ($\lambda=4$), the column strengthened with the new technique ($\lambda 4$ -SC) has
299 presented a notable higher performance in terms of the compressive strength and its corresponding
300 axial deformation compared to the other strengthened columns. When compared to the corresponding
301 reference column, the increase in terms of compressive strength provided by the SC technique was
302 approximately 25% and 32% in the columns' group of $\lambda=2.0$ and $\lambda=4.0$, respectively, while the
303 conventional strengthening techniques only assured an increase ranging from 7% to 23%. However,
304 due to the very brittle rupture occurred in the loading zone of the $\lambda 4$ -FW column, an abrupt load
305 decay has occurred. To avoid this type of premature failure, or at least postpone its occurrence for
306 larger axial deformation, it seems important to increase the confinement stiffness of the column's
307 extremities.

308 A comparison of the axial stress versus the CFRP strain (ε_f) for the strengthened columns is
309 illustrated in Fig. 10, while Fig. 11 compares the column's axial strain with ε_f (in this last figure the
310 values are only presented up to the peak load of the column). The position of the strain gauge where
311 the ε_f is evaluated is presented in the corresponding figures. For the same level of stress, it can be
312 seen that the CFRP strain in the columns strengthened according to the new technique was higher
313 compared to the CFRP strain in the columns strengthened with the other techniques. In the case of the
314 columns with $\lambda=2$ this has only occurred above the axial deformation corresponding to the
315 compressive strength of the reference column ($\lambda 2$ -REF), Fig. 11b. On the other hand, in the columns
316 with $\lambda=4$ this phenomenon is visible since the beginning of the tests. These larger values of strain
317 suggest that the confinement effectiveness provided by the CFRP strips was higher when using the
318 new strengthening technique, and the relative confinement effectiveness of the SC technique seems as

319 higher as larger is λ . The maximum CFRP strain values recorded in the strain gauge localized at mid-
320 depth of the strengthened columns ($\varepsilon_{f\max}$) are indicated in Table 3. At the moment of failure of the
321 strengthened columns, $\varepsilon_{f\max}$ was higher in the columns strengthened with the SC technique than with
322 the other two techniques, indicating that the new technique mobilizes more effectively the
323 confinement potential of the CFRP. However, apart the $\varepsilon_{f\max}$ value registered in the $\lambda 1$ -FW (8.34‰),
324 the values of $\varepsilon_{f\max}$ recorded in the other columns were relatively small, which is justified by the
325 occurrence of failure at the top extremity of these columns, preventing the full exploitation of the
326 confinement effectiveness of the adopted strengthening configurations.

327

328 **3.4 Effect of cross-section aspect ratio on the confinement performance of the adopted** 329 **strengthening techniques**

330 The axial stress-strain relationship (σ_c - ε_c) for each group of columns with different cross section
331 aspect ratio (λ) is shown in Fig. 12. In all the four groups of columns, the compressive strength and
332 the ultimate axial strain have decreased with the increase of λ . Due to the identical strength class for
333 the concrete of the tested columns, and the equal arrangement for the steel reinforcement and CFRP
334 systems, the initial stiffness of the σ_c - ε_c response was similar in each group of columns. Fig. 12a
335 shows that the amplitude of the axial deformation in the σ_c - ε_c softening stage increases with λ in the
336 REF columns. In the group of columns strengthened with the FW technique (Fig. 12b), the ductility of
337 the σ_c - ε_c response (indicator based on the area under the σ_c - ε_c up to the column's failure) has
338 significantly increased with the decrease of λ . All the columns of the group strengthened by the PW
339 technique (Fig. 12c) have presented a post-peak σ_c - ε_c softening stage. This stage is formed by an
340 initial more abrupt stress-decay branch, where the σ_c/ε_c softening gradient has decreased with the
341 decrease of λ (more ductile behavior), followed by a stage with a more smooth σ_c/ε_c softening
342 gradient, almost equal in all the columns of this group. Finally, the group of columns strengthened
343 with the SC technique (Fig. 12d) clearly demonstrates that the decrease of compressive strength with
344 the increase of λ was much lower than the decrease registered in the other groups of columns,
345 although the deformation capacity and post-peak resistance has decreased significantly with the
346 increase of λ . As already indicated, this fact is justified by the quite different failure modes observed
347 in these two columns.

348 A comparison of strength gain for all strengthened columns is illustrated in Fig.13. The strength gain
349 was calculated by the ratio between the compressive strength of a strengthened and its corresponding
350 reference column ($\sigma_{cc}^{Str} / \sigma_{cc}^{Ref}$). It can be observed that when the cross-section aspect ratio increases,
351 the strength gain of the fully-wrapped columns significantly decreases. The strength gain values
352 corresponding to the fully-wrapped columns (FW) were 1.67, 1.23 and 1.07 for the cross-section

353 aspect ratio of 1, 2 and 4, respectively. Regarding the strength gain of the partially-wrapped columns
354 (PW), the observed values were relatively constant, since they have varied between 1.07-1.13 for this
355 strengthening technique. Finally, the new technique (SC) provided an increase of strength gain with
356 the increase of the cross-section aspect ratio, since $\sigma_{cc}^{Str} / \sigma_{cc}^{Ref}$ was 1.25 and 1.32 for the column of
357 cross-section aspect ratio of 2 and 4, respectively. These results indicate that, despite the smaller
358 content of CFRP applied in the SC technique compared to the FW technique, the SC is more effective
359 for RC of relatively large cross-section aspect ratio.

360

361 **4. ASSESSMENT THE APPLICABILITY OF EXISTING DESIGN RECOMMENDATIONS**

362 To predict the load carrying capacity of the tested columns, the following three existing models were
363 selected: *fib* Bulletin 14 [21]; CNR-DT 200 [22]; and ACI 440.2R-08 [1]. A summary of the
364 corresponding formulation is provided in Appendix. All these models consider only the confinement
365 contribution from external FRP wrapping (the contribution from steel hoops is not taken into
366 account). The *fib* Bulletin 14 and CNR-DT 200 models adopt a vertical efficiency coefficient to
367 simulate the effective lateral confining pressure of partially FRP-confined columns, which is not the
368 case of ACI 440.2R-08 formulation that was prepared exclusively for full wrapping arrangement. In
369 order to extend the applicability of the ACI formulation for RC columns partially confined with FRP
370 systems, the equation providing the effective lateral confining pressure of partially FRP-confined
371 columns in ACI code is modified by introducing the vertical efficiency coefficient obtained according
372 to CNR-DT 200 recommendations (Eq. A.16).

373 To apply these models for the prediction of the concrete strength of columns strengthened according
374 to the SC technique, a rectangular cross section is considered as a parallel series of “cells” of almost
375 square section, as schematically shown in Fig. 14. According to the SC technique the number of
376 divisions (n_d) in the larger cross section dimension provided by the mechanical components of this
377 technique should assure “cells” of almost square cross section ($n_d \approx h/b$). Therefore, the compressive
378 strength of a rectangular column strengthened according to the SC technique is the same as the
379 compressive strength of a column of square cross section of $b \approx h/n_d$ edge. At the present stage, the
380 favorable effect in terms of lateral confinement provided by the prestress applied to the CFRP strips in
381 the SC technique is not taken into account, since deeper knowledge on the long term values of this
382 prestress must be known, as well as its spatial distribution, which is an ongoing research.

383 The analytical results obtained from the adopted guidelines are presented in Table 4. For conventional
384 strengthening techniques with the cross section ratio equal to 1 and 2, the *fib* Bulletin 14 (“Exact
385 approach”), CNR-DT 200 and ACI.2R-08 predict with good accuracy the confined concrete strength
386 values registered experimentally, while the *fib* Bulletin 14 (“Approximate approach”) provides quite
387 conservative predictions. It is verified that the modification introduced in the ACI.2R-08 model in

388 order to extend its applicability to partially confinement arrangements seems adequate since it
389 provides a similar level of accuracy in FW and PW columns.

390 The *fib* Bulletin 14 and CNR-DT 200 models are not prepared for predicting the concrete strength of
391 confined columns of cross-section ratio higher than 3.6, since the coefficient of horizontal efficiency
392 (Eq. A.15) becomes a negative value. However, the applicability of ACI.2R-08 model is not limited
393 by this condition, and the results reported in Table 4 show a satisfactory level of prediction for the
394 columns of $\lambda=4$, for both FW and PW.

395 The results in Table 4 also demonstrate that the approach adopted in Fig. 14 for the SC technique
396 allows all the considered formulations (apart from *fib* Bulletin 14 model with the approximate
397 approach) to predict with good accuracy the compressive strength of the tested columns strengthened
398 with the proposed technique: -17.56% to -5.48% and -7.48% to 3.56% for the columns with cross-
399 section ratio of 2 and 4, respectively.

400

401 5. CONCLUSIONS

402 In this work, a new technique for the confinement of rectangular reinforced concrete (RC) columns is
403 presented and its effectiveness was assessed by performing an experimental program. The effect of
404 the cross-section aspect ratio on the confinement effectiveness provided by different strengthening
405 techniques was investigated. For the cross-section aspect ratio ($\lambda=h/b$) of the columns the values of 1,
406 2 and 4 were adopted, corresponding to column's cross section of $120\times 120\text{ mm}^2$, $240\times 120\text{ mm}^2$ and
407 $480\times 120\text{ mm}^2$, respectively. Four types of columns were tested: 1) reference, without any type of
408 confinement (REF); 2) fully-wrapped (FW); 3) partially wrapped (PW); and 4) columns strengthened
409 according to the proposed technique, designated by strip constriction (SC). The relevant results can be
410 summarized as follows:

411 (1) All the strengthened columns showed an increase of the load carrying capacity and axial
412 deformation performance compared with their corresponding reference columns.

413 (2) When compared to the corresponding reference column, the increase in terms of strength gain
414 provided by the FW confinement was approximately 67%, 23% and 7% in the columns of $\lambda=1$, $\lambda=2$
415 and $\lambda=4$, respectively. Regarding the PW confinement configuration, the strength gain was
416 approximately constant in the tested columns (in between 7% and 13%). The proposed SC technique
417 provided an increase of 25% and 32 % in the columns of $\lambda=2$ and $\lambda=4$, respectively.

418 (3) The increase of load carrying capacity per quantity of CFRP strengthening material of the SC
419 technique is higher than the other strengthening techniques, indicating that the SC technique is not
420 only technically efficient, but also cost competitive.

421 (4) In RC columns of highest cross-section aspect ratio ($\lambda=4$), the SC technique has provided a higher
422 increase of compressive strength and axial deformability compared to the other conventional

423 strengthening techniques. For the column's group of $\lambda=2$, the SC technique was the most effective in
424 terms of compressive strength, but the FW technique has provided the highest axial deformation.

425 (5) The experimental results revealed that for the same level of column's axial stress, the maximum
426 CFRP strain in the SC columns was higher than in the columns strengthened with the other two
427 considered strengthening techniques.

428 (6) The effect of cross-section aspect ratio plays an important role on the performance of strengthened
429 RC columns. For all strengthened groups of columns with different λ , the compressive strength and
430 ultimate axial strain have decreased with the increase of the cross-section aspect ratio. However, the
431 columns strengthened according to SC technique showed a lower decrease of compressive strength
432 with the increase of λ compared to the other strengthening groups of columns.

433 (7) The predictive performance of *fib* Bulletin 14 (*Exact and approximate approaches*), CNR-DT 200
434 and ACI.2R-08 for the estimation of the compressive strength of the investigated strengthening
435 techniques was assessed. Apart from the "*approximate approach*" of *fib* Bulletin 14, which estimated
436 too conservative values, the remaining analytical models have provided satisfactory predictions for
437 the columns with $\lambda=1$ and $\lambda=2$. The ACI.2R-08 model is, amongst the considered ones, the only one
438 that can predict the compressive strength of confined columns of $\lambda>4$, although its applicability was
439 restricted to FW confinement configurations. This formulation was extended to PW configurations
440 with acceptable predictive performance.

441 (8) By idealizing a rectangular cross section of a column strengthened with the proposed SC technique
442 as a set of parallel square cells, *fib*, *CNR* and *ACI* models were adapted for predicting the compressive
443 strength of SC strengthened columns. The obtained results evidence good predictive performance.

444

445 6. ACKNOWLEDGEMENTS

446 The first author would like to thank Erasmus Mundus Programme and TecMinho to provide financial
447 and scholarship supports. The support from the FCT in the scope of PTDC/ECM-EST/1882/2014
448 project is also acknowledged. Moreover, the authors would like to thank the collaboration of Casais
449 and CiviTest companies for the collaboration on the preparation of the RC columns, and Clever
450 Reinforcement Company for providing the CFRP sheets and adhesives. Also gratefully acknowledge
451 the technicians of laboratory of the structural division of the Department of Civil Engineering of
452 Minho University.

453

454 7. REFERENCES

- 455 [1] ACI 440.2R-08. Guide for the design and construction of externally bonded FRP systems for
456 strengthening existing structures. American Concrete Institute 2008.
- 457 [2] Nisticò N, Pallini F, Rousakis T, Wu YF, Karabinis A. Peak strength and ultimate strain prediction
458 for FRP confined square and circular concrete sections. *Compos Part B Eng* 2014;67:543–54.

- 459 [3] Mirmiran A, Shahawy M, Samaan M, Echary H El, Mastrapa JC, Pico O, et al. Effect of column
460 parameters on FRP-confined concrete. *J Compos Constr* 1998;2:175–85.
- 461 [4] Rochette P, Labossière P. Axial Testing of Rectangular Column Models Confined with
462 Composites. *J Compos Constr* 2000;4:129–36.
- 463 [5] Chaallal O, Shahawy M, Hassan M. Performance of Axially Loaded Short Rectangular Columns
464 Strengthened with Carbon Fiber-Reinforced Polymer Wrapping. *J Compos Constr* 2003;7:200–8.
- 465 [6] Harajli MH. Axial stress-strain relationship for FRP confined circular and rectangular concrete
466 columns. *Cem Concr Compos* 2006;28:938–48.
- 467 [7] Colajanni P, Fossetti M, MacAluso G. Effects of confinement level, cross-section shape and
468 corner radius on the cyclic behavior of CFRCM confined concrete columns. *Constr Build Mater*
469 2014;55:379–89.
- 470 [8] Faustino P, Chastre C, Paula R. Design model for square RC columns under compression confined
471 with CFRP. *Compos Part B Eng* 2014;57:187–98.
- 472 [9] Lam L, Teng JG. Design-oriented stress-strain model for FRP-confined concrete in rectangular
473 columns. *J Reinf Plast Compos* 2003;22:1149–86.
- 474 [10] Farghal OA. Structural performance of axially loaded FRP-confined rectangular concrete
475 columns as affected by cross-section aspect ratio. *HBRC J* 2016.
- 476 [11] Yang X, Wei J, Nanni A, Dharani LR. Shape Effect on the Performance of Carbon Fiber
477 Reinforced Polymer Wraps. *J Compos Constr* 2004;8:444–51.
- 478 [12] Al-Salloum YA. Influence of edge sharpness on the strength of square concrete columns
479 confined with FRP composite laminates. *Compos Part B Eng* 2007;38:640–50.
- 480 [13] Wang LM, Wu YF. Effect of corner radius on the performance of CFRP-confined square
481 concrete columns: Test. *Eng Struct* 2008;30:493–505.
- 482 [14] Benzaid R, Chikh N, Mesbah H. Behaviour of square concrete column confined with GFRP
483 composite wrap. *J Civ Eng Manag* 2008;14:115–20.
- 484 [15] Abbasnia R, Ahmadi R, Ziaadiny H. Effect of confinement level, aspect ratio and concrete
485 strength on the cyclic stress-strain behavior of FRP-confined concrete prisms. *Compos Part B*
486 *Eng* 2012;43:825–31.
- 487 [16] Cole C. Confinement Characteristics of Rectangular FRP-Jacketed RC Columns. *Fifth Int. Symp.*
488 *Fiber Reinf. Polym. Reinf. Concr. Struct. (FRPRCS-5)*, July 16-18, 2001, Cambridge, UK: 2001,
489 p. 823–32.
- 490 [17] Wu YF, Wei YY. Effect of cross-sectional aspect ratio on the strength of CFRP-confined
491 rectangular concrete columns. *Eng Struct* 2010;32:32–45.
- 492 [18] Hadi MNS, Pham TM, Lei X. New Method of Strengthening Reinforced Concrete Square
493 Columns by Circularizing and Wrapping with Fiber-Reinforced Polymer or Steel Straps. *J*
494 *Compos Constr* 2013;17:229–38.

$$515 \quad \sigma_{ly} = K_{confy} \varepsilon_{ju}; K_{confy} = \rho_{jy} k_e E_f; \rho_{jy} = \frac{2b_f n t_f}{p_f h} \quad (A.6)$$

$$516 \quad k_e = k_H k_V \quad (A.7)$$

$$517 \quad k_H = 1 - \frac{(b - 2r_c)^2 + (h - 2r_c)^2}{3A_g (1 - \rho_{sg})} \quad (A.8)$$

$$518 \quad k_V = \left(1 - \frac{p'_f}{2b}\right) \quad (A.9)$$

519 where f_{cc} is the compressive strength of FRP-confined concrete; f_{co} is the compressive strength of
520 unconfined concrete; f_l is the equivalent lateral confining pressure; σ_{lx} and σ_{ly} are the lateral
521 confining pressure acting perpendicular to core dimensions h and b , respectively; b is the smaller
522 dimension of the column cross section; h is the larger dimension of the column cross section; r_c is
523 the corner radius of the cross section; K_{confx} and K_{confy} are the stiffness of the FRP wrapping in x and
524 y direction; ε_{ju} is the effective tensile failure strain of the FRP wrapping; E_f is the modulus of the
525 FRP wrapping; ρ_{jx} and ρ_{jy} are the volumetric ratio of transverse confining reinforcement in the x
526 and y direction, respectively; b_f is the width of FRP strip; n is the number of FRP layers; t_f is the
527 thickness of FRP per one layer; p_f is the center-to-center spacing of FRP strips; A_g is the gross area
528 of the cross section; ρ_{sg} is the longitudinal steel reinforcement ratio; k_e is the confinement
529 effectiveness coefficient; k_H is the coefficient of horizontal efficiency; k_V is the coefficient of
530 vertical efficiency. For RC confined member with continuous FRP wrapping, it is assumed that $k_V =$
531 1; and p'_f is the clear spacing between FRP strips

532

533 *CNR-DT 200/2004 proposal guideline for FRP-confined concrete (CNR-DT 200, 2004) [22]*

$$534 \quad \frac{f_{cc}}{f_{co}} = 1 + 2.6 \left(\frac{f_{l,eff}}{f_{co}} \right)^{\frac{2}{3}} \quad (A.10)$$

$$535 \quad f_{l,eff} = k_e f_l \quad (A.11)$$

$$536 \quad f_l = \frac{1}{2} \rho_f E_f \varepsilon_{fd,rid}; \rho_f = \frac{2n t_f (b + h) b_f}{b h p_f} \quad (A.12)$$

$$537 \quad \varepsilon_{fd,rid} = \min \left\{ \eta_a \varepsilon_{fk} / \gamma_f; 0.004 \right\} \quad (A.13)$$

$$538 \quad k_e = k_H k_V k_\alpha \quad (A.14)$$

$$539 \quad k_H = 1 - \frac{(b-2r_c)^2 + (h-2r_c)^2}{3A_g} \quad (\text{A.15})$$

$$540 \quad k_V = \left(1 - \frac{\rho_f'}{2b}\right) \quad (\text{A.16})$$

$$541 \quad k_\alpha = \frac{1}{1 + (\tan \alpha_f)^2} \quad (\text{A.17})$$

542 where $f_{l,eff}$ is the effective confinement lateral pressure; ρ_f is the geometric strengthening ratio as a
 543 function of section shape and FRP configuration (continuous or discontinuous wrapping); $\varepsilon_{fd,rid}$ is the
 544 reduced FRP design strain; η_a is the environmental conversion factor for the external exposure
 545 conditions of FRP systems (=0.85); γ_f is the partial factor for FRP material (=1.10); ε_{fk} is the
 546 characteristic strain at failure; k_α is the coefficient of fiber orientation; and α_f is the angle of fibers.

547

548 *ACI 440.2R-08 proposal guideline for FRP-confined concrete (ACI, 2004) [1]*

$$549 \quad f'_{cc} = f_{co} + \psi_f 3.3k_e f_l \quad (\text{A.18})$$

$$550 \quad f_l = \frac{2E_f n t_f \varepsilon_{fe}}{D} \quad (\text{A.19})$$

$$551 \quad \varepsilon_{fe} = k_e \varepsilon_{fu} \quad (\text{A.20})$$

$$552 \quad D = \sqrt{b^2 + h^2} \quad (\text{A.21})$$

$$553 \quad k_e = k_H k_V \quad (\text{A.22})$$

$$554 \quad k_H = \frac{A_e}{A_c} \left(\frac{b}{h}\right)^2 \quad (\text{A.23})$$

$$555 \quad \frac{A_e}{A_c} = \frac{1 - \frac{\left[\left(\frac{b}{h}\right)(h-2r_c)^2 + \left(\frac{h}{b}\right)(b-2r_c)^2\right]}{3A_g} - \rho_{sg}}{1 - \rho_{sg}} \quad (\text{A.24})$$

556 where ψ_f is an additional reduction factor based on the committee's judgment (=0.95); ε_{fe} is the
 557 effective strain level in the FRP at failure; k_e is the FRP strain efficiency factor (=0.586); ε_{fu} is the
 558 ultimate tensile strain of FRP material; D is the diagonal of rectangular cross section; k_V is the
 559 coefficient of vertical efficiency (obtained according to CNR-DT 200 proposal guideline).

FIGURES

List of Figures:

Fig. 1 - Geometry, reinforcement, and strengthening configuration for the series of RC columns with cross-sectional aspect ratio of: a) 1; b) 2; and c) 4 (dimension in mm)

Fig. 2 - Schematic representation of the new proposed technique

Fig. 3 - Representation of the prestress application on the CFRP strips

Fig. 4 - Strain gauge positioning (red mark) and test setup (dimension in mm)

Fig. 5 - Failure modes of the columns with cross-section aspect ratio (λ) equal to 1

Fig. 6 - Failure modes of the columns with cross-section aspect ratio (λ) equal to 2

Fig. 7 - Failure modes of the columns with cross-section aspect ratio (λ) equal to 4

Fig. 8 - Axial stress versus axial strain relationship recorded in the λ 1-REF column for the following three measuring strokes: 200, 600 and 1060 mm

Fig. 9 - Axial stress versus axial strain relationship in the RC columns of cross-section aspect ratio (λ) of: a) 1; b) 2; and c) 4

Fig. 10 - Axial stress versus CFRP strain relationship in the RC columns of cross-section aspect ratio (λ) of: a) 1; b) 2; and c) 4

Fig. 11 - Column's axial strain versus CFRP strain relationship in the RC columns of cross-section aspect ratio (λ) of: a) 1; b) 2; and c) 4

Fig. 12 - Axial stress-strain relationship for all types of columns with different cross-section aspect ratios

Fig. 13 - Strength gain of the strengthened columns versus cross-section aspect ratios

Fig. 14 - Effective confinement area of rectangular sections provided by the proposed (SC) technique

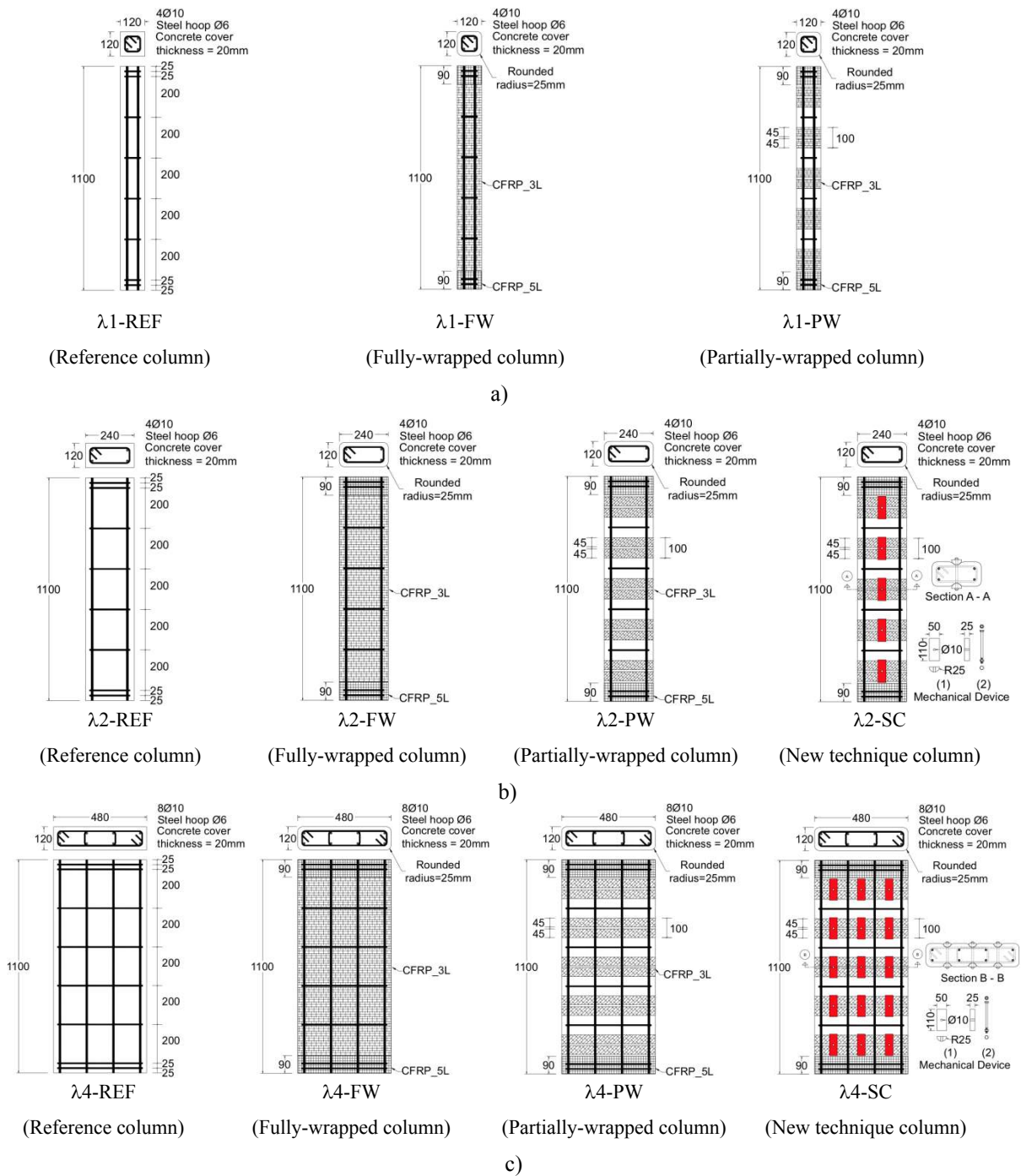


Fig. 1 - Geometry, reinforcement, and strengthening configuration for the series of RC columns with cross-sectional aspect ratio of: a) 1; b) 2; and c) 4 (dimension in mm)

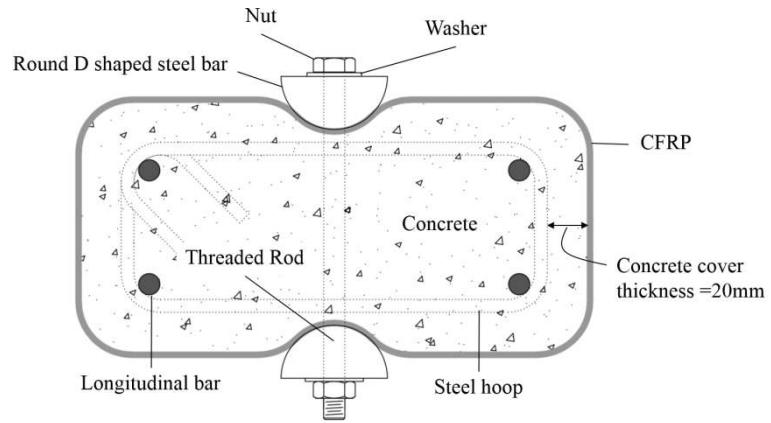


Fig. 2 - Schematic representation of the new proposed technique



Fig. 3 - Representation of the prestress application on the CFRP strips

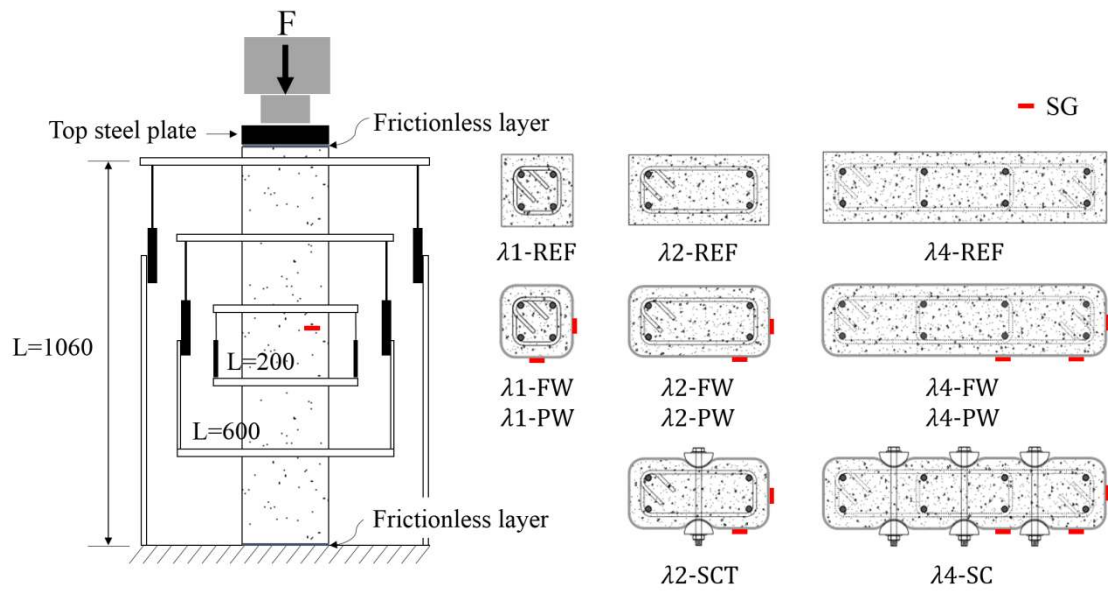
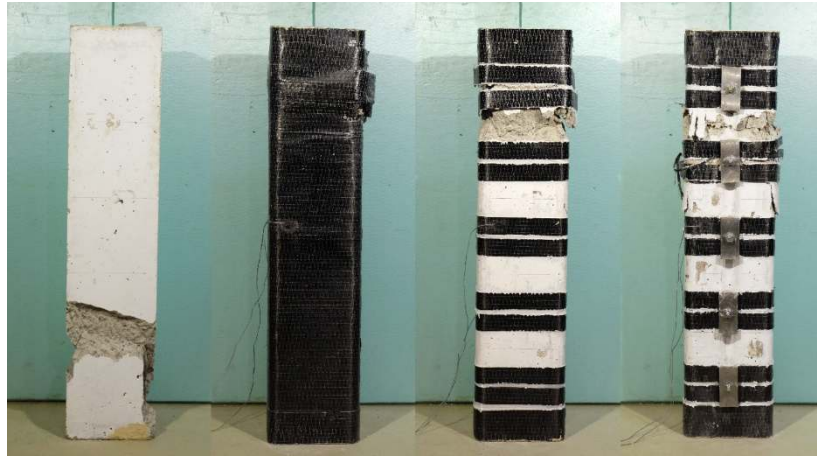


Fig. 4 - Strain gauge positioning (red mark) and test setup (dimensions in mm)



(a) λ_1 -REF (b) λ_1 -FW (c) λ_1 -PW

Fig. 5 - Failure modes of the columns with cross-section aspect ratio (λ) equal to 1



(a) $\lambda 2$ -REF

(b) $\lambda 2$ -FW

(c) $\lambda 2$ -PW

(d) $\lambda 2$ -SC

Fig. 6 - Failure modes of the columns with cross-section aspect ratio (λ) equal to 2



(a) $\lambda 4$ -REF

(b) $\lambda 4$ -FW

(c) $\lambda 4$ -PW

(d) $\lambda 4$ -SC

Fig. 7 - Failure modes of the columns with cross-section aspect ratio (λ) equal to 4

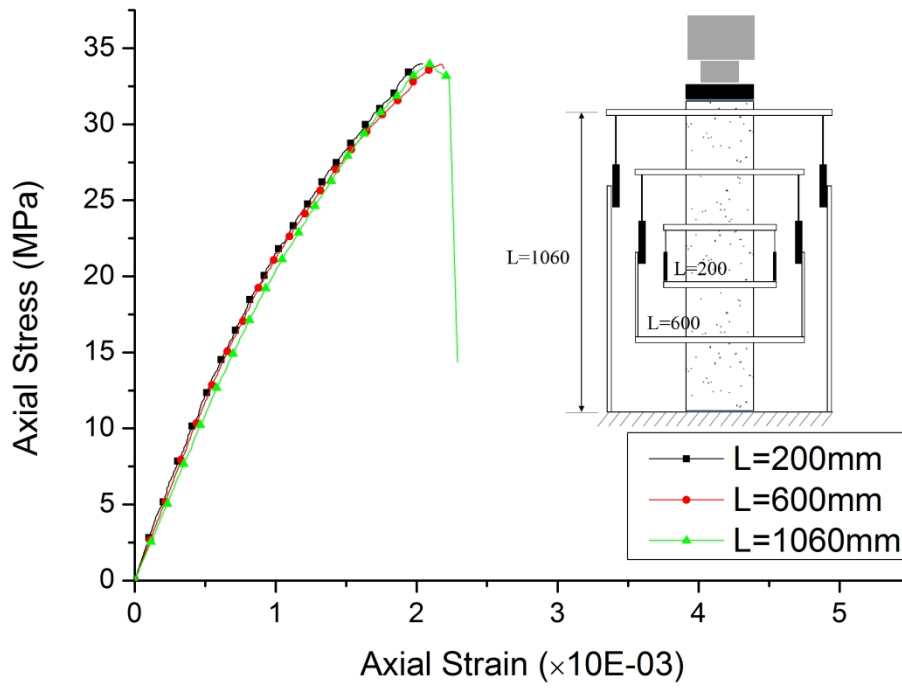


Fig. 8 - Axial stress versus axial strain relationship recorded in the $\lambda 1$ -REF column for the following three measuring strokes: 200, 600 and 1060 mm

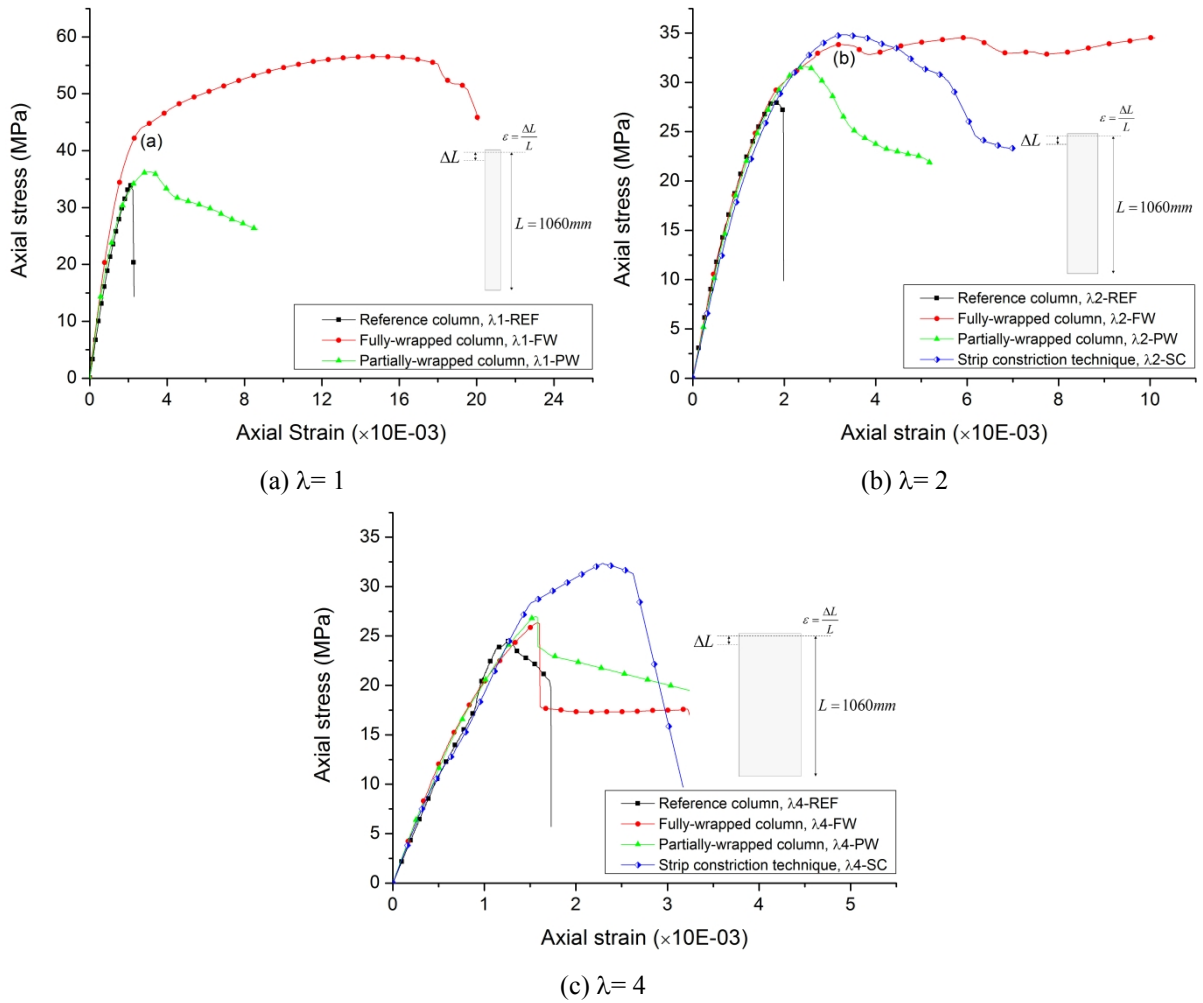


Fig. 9 - Axial stress versus axial strain relationship in the RC columns of cross-section aspect ratio (λ) of: a) 1; b) 2; and c) 4

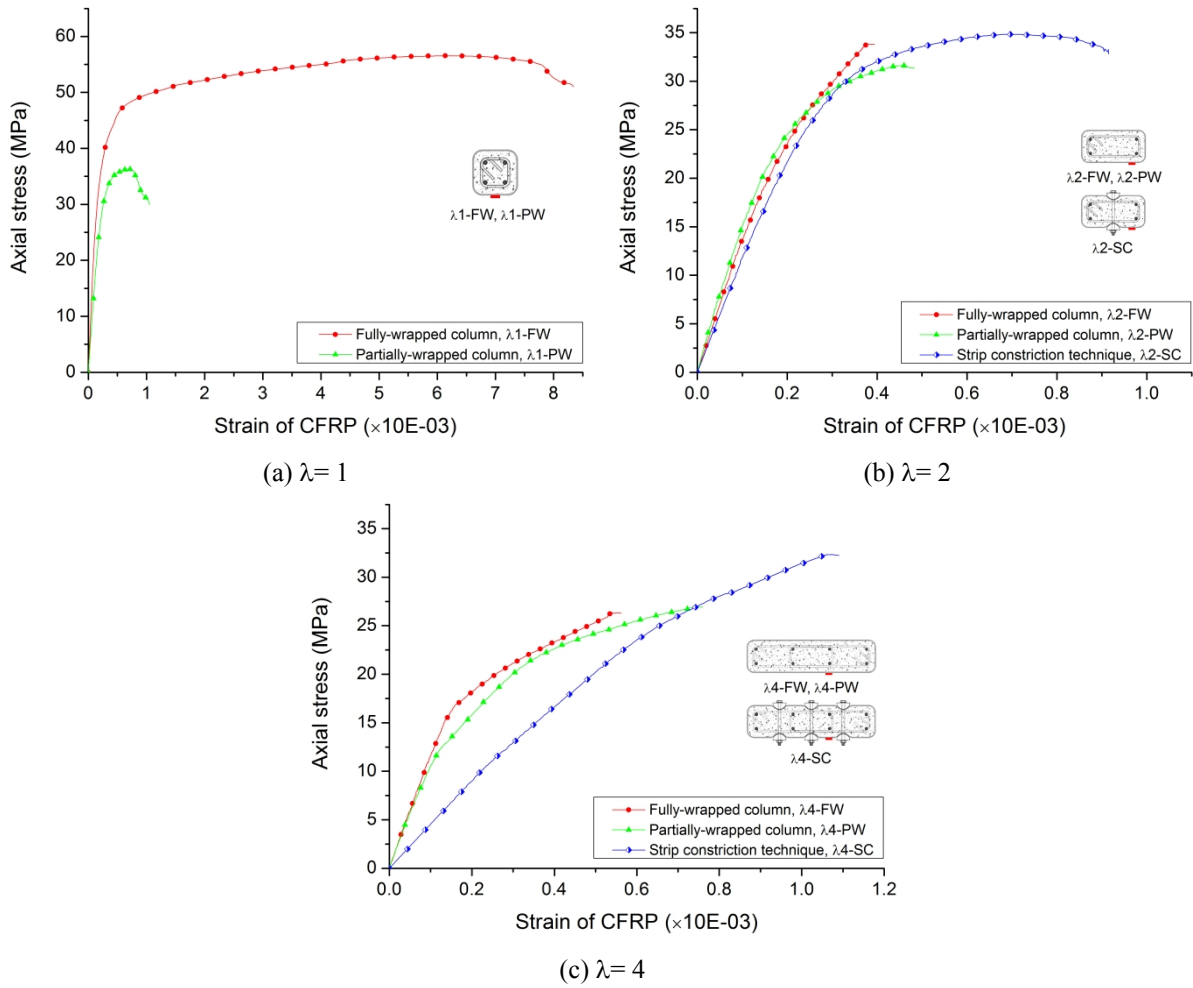


Fig. 10 - Axial stress versus CFRP strain relationship in the RC columns of cross-section aspect ratio (λ) of: a) 1; b) 2; and c) 4

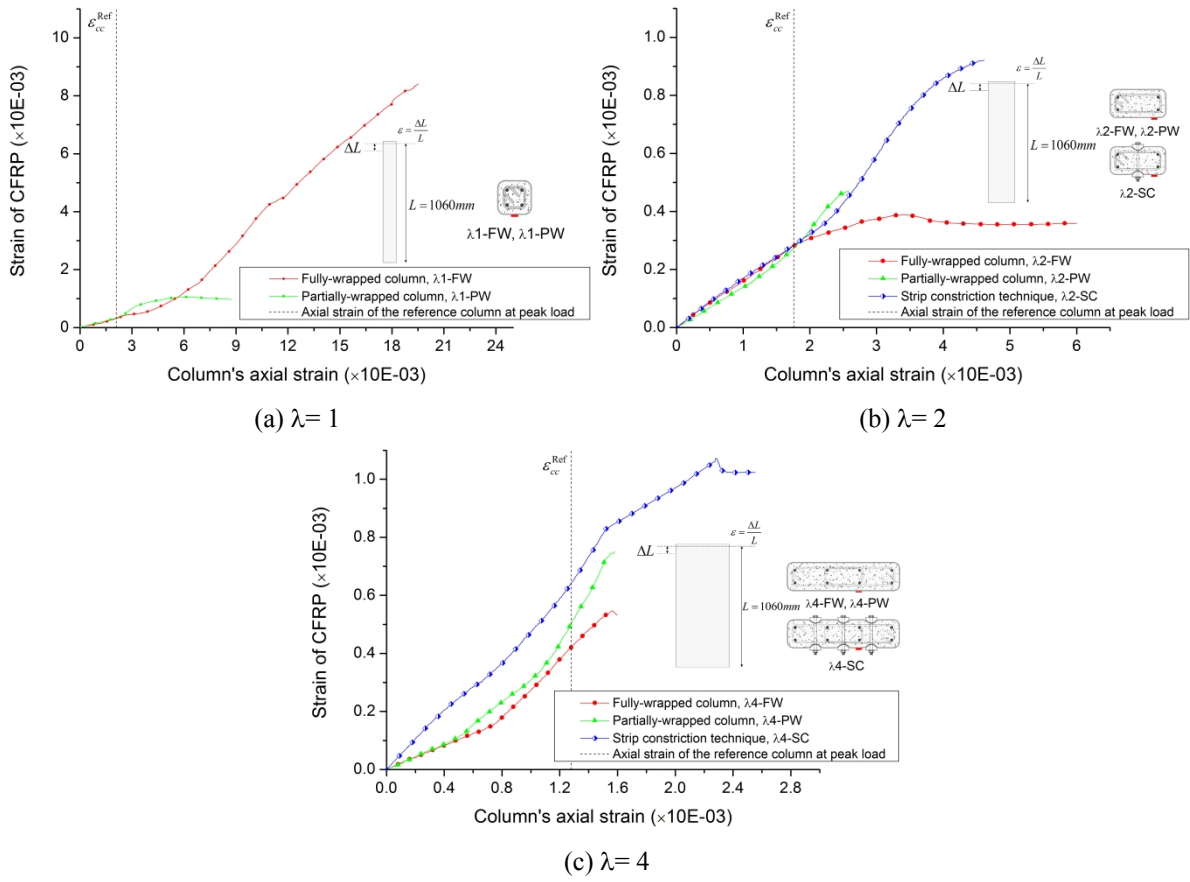
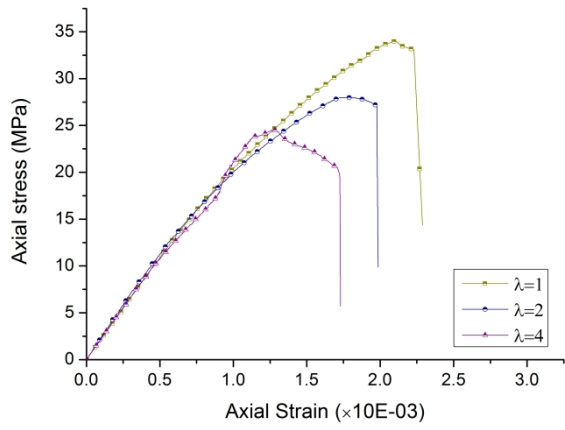
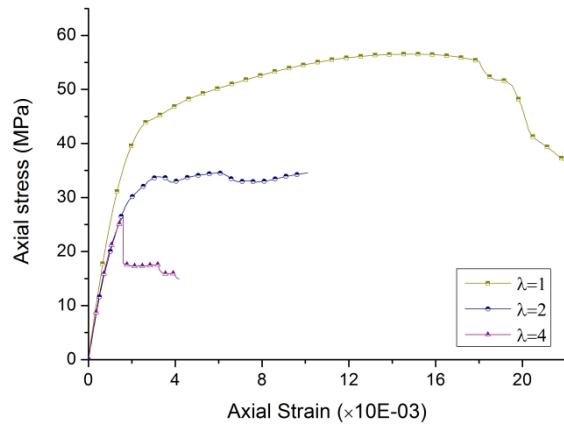


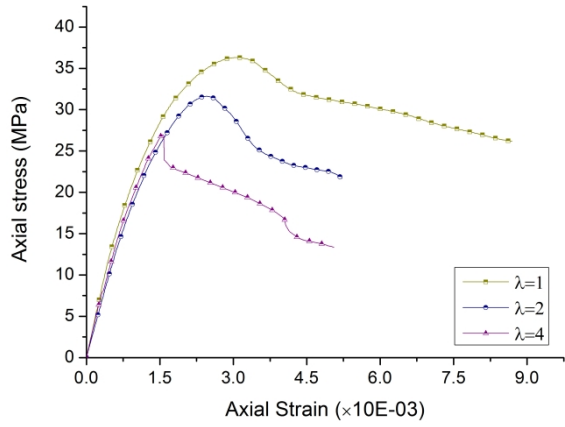
Fig. 11 - Column's axial strain versus CFRP strain relationship in the RC columns of cross-section aspect ratio (λ) of: a) 1; b) 2; and c) 4



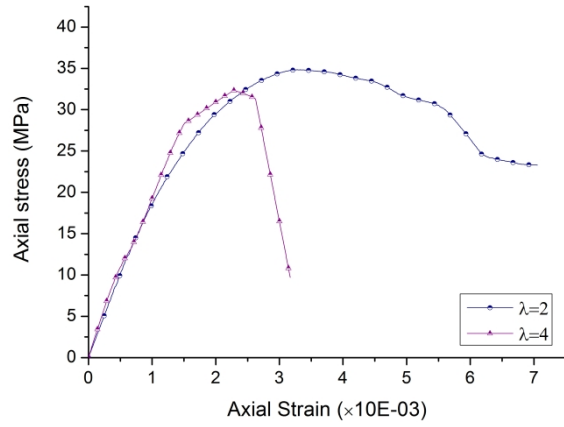
(a) Reference columns (REF)



(b) Fully-wrapped (FW) technique



(c) Partially-wrapped (PW) technique



(d) Strip constriction (SC) technique

Fig. 12 - Axial stress-strain relationship for all types of columns with different cross-section aspect ratio

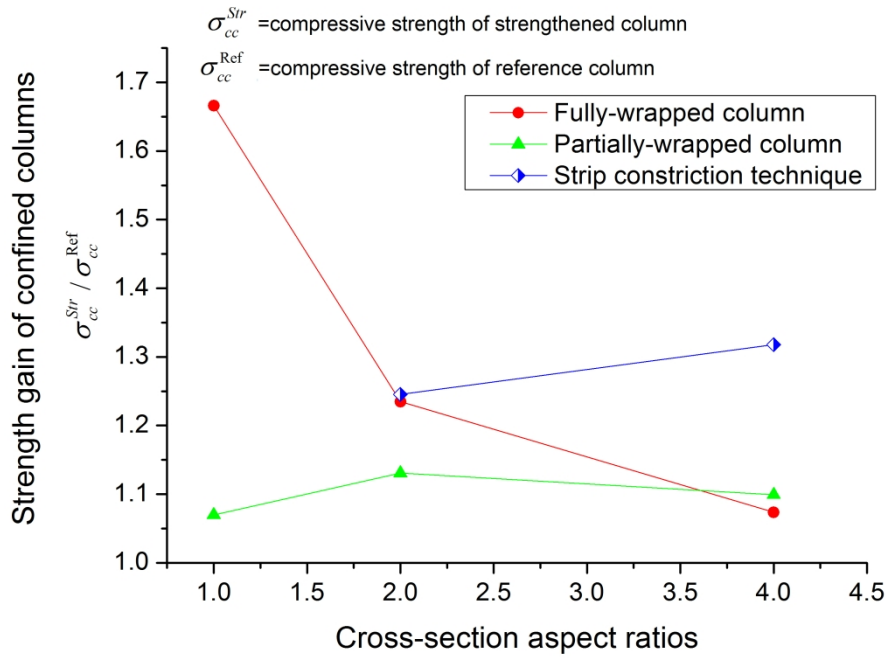


Fig. 13 - Strength gain of the strengthened columns versus cross-section aspect ratios

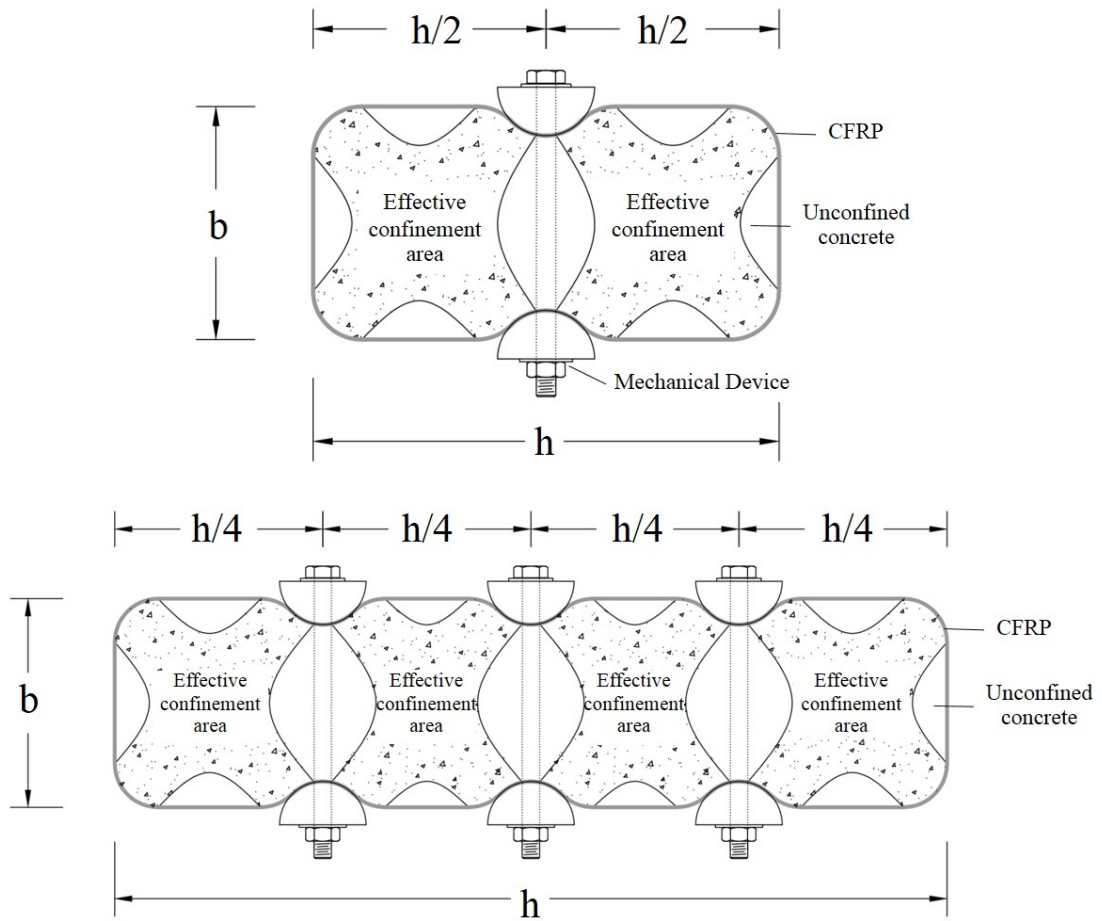


Fig. 14 - Effective confinement area of rectangular sections provided by the proposed (SC) technique

TABLES

List of Tables:

Table 1 - Mechanical properties of CFRP (S&P C-sheet 240)

Table 2 - Mechanical properties of epoxy adhesive (S&P Resin 55)

Table 3 - Summary of experimental results for all columns

Table 4 - Comparison of results obtained from experimental tests and analytical models for RC columns of square and rectangular cross section

Table 1 - Mechanical properties of CFRP (S&P C-sheet 240)

Property	Value
Tensile strength (MPa)	3800
Tensile modulus (GPa)	240
Elongation at rupture (%)	1.55
Density (g/cm ³)	1.7
Thickness (mm/ply)	0.117

Table 2 - Mechanical properties of epoxy adhesive (S&P Resin 55)

Property	Value
Density (Kg/l)	1.11
Mixing ratio by weight (resin to hardener)	2:1
Tensile strength at 14 days (MPa)	35.8
Elongation at failure at 14 days (%)	2.3
Modulus of elasticity at 14 days(MPa)	2581.8

Table 3 - Summary of experimental results for all columns

Column designation	$\lambda=h/b$	A_{eff} (mm ²)	P_{max} (kN)	σ_{cc} (MPa)	ε_{cc} (‰)	ε_{fmax} (‰)	ΔF_{max} (%)	$\Delta \bar{\varepsilon}_{cc}$ (%)	A_{CFRP} (m ²)	$\Delta F_{max} / A_{CFRP}$ (%/m ²)
$\lambda 1$ -REF		14400.00	488.70	33.94	2.09	-	-	-	-	-
$\lambda 1$ -FW	1	13863.50	783.85	56.54	14.84	8.34	66.60	610.81	1.78	37.36
$\lambda 1$ -PW		13863.50	503.32	36.31	3.06	1.05	6.98	46.30	1.10	6.37
$\lambda 2$ - REF		28800.00	805.45	27.97	1.76	-	-	-	-	-
$\lambda 2$ - FW	2	28263.50	976.10	34.54	10.04	0.39	23.49	469.45	2.66	8.83
$\lambda 2$ - PW		28263.50	893.68	31.62	2.45	0.48	13.06	38.97	1.64	7.98
$\lambda 2$ -SC		27192.30	947.11	34.83	3.28	0.92	24.54	86.05	1.64	15.00
$\lambda 4$ - REF		57600.00	1413.08	24.53	1.28	-	-	-	-	-
$\lambda 4$ - FW	4	57063.50	1502.92	26.34	1.58	0.56	7.36	24.08	4.42	1.67
$\lambda 4$ - PW		57063.50	1538.95	26.97	1.55	0.76	9.93	21.57	2.72	3.66
$\lambda 4$ - SC		53849.90	1741.45	32.34	2.29	1.09	31.82	79.61	2.72	11.72

Table 4 - Comparison of results obtained from experimental tests and analytical models for RC columns of square and rectangular cross section

Column designation	Experimental result, f_{cc}^{exp} (MPa)	Analytical models, f_{cc}^{anal}				$\frac{f_{cc}^{anal} - f_{cc}^{exp}}{f_{cc}^{exp}} \times 100$			
		<i>fib</i>		CNR- DT 200	ACI	<i>fib</i>		CNR- DT-200	ACI
		Approx. (MPa)	Exact. (MPa)	(MPa)	(MPa)	Approx. (%)	Exact. (%)	(%)	(%)
$\lambda 1$ -REF	25.16	-	-	-	-	-	-	-	-
$\lambda 1$ -FW	47.42	32.09	41.11	39.51	42.81	-47.77	-15.34	-20.02	-10.76
$\lambda 1$ -PW	26.71	15.71	25.50	26.68	28.42	-70.04	-4.76	-0.13	6.00
$\lambda 2$ - REF	24.36	-	-	-	-	-	-	-	-
$\lambda 2$ - FW	29.87	25.09	33.83	32.77	24.04	-19.03	11.72	8.86	-24.23
$\lambda 2$ - PW	26.92	12.82	23.61	24.61	22.03	-109.96	-14.01	-9.37	-22.18
$\lambda 2$ -SC	29.98	15.71	25.50	26.68	28.42	-90.82	-17.56	-12.36	-5.48
$\lambda 4$ - REF	21.93	-	-	-	-	-	-	-	-
$\lambda 4$ - FW	23.04	N/A	N/A	N/A	21.38	N/A	N/A	N/A	-7.75
$\lambda 4$ - PW	23.72	N/A	N/A	N/A	21.13	N/A	N/A	N/A	-12.27
$\lambda 4$ - SC	27.41	15.71	25.50	26.68	28.42	-74.46	-7.48	-2.73	3.56

N/A = not available